배합고무와 나노구리 박판으로 구성된 복합체에서의 접착계면의 미시적 분석

전경수*, 정승원, 최석주[1]
남도대학 토목환경과, [1]금호타이어㈜ 컴파운드 개발팀
(gjeon@damyang.ac.kr*)

Microscopic analysis of adhesion interphase in the composite made up of rubber compound and nano-copper-coated iron plate

Gyung Soo Jeon*, Seung Won Jeong, Seok Ju Choi[1]
Department of Civil & Environmental Engineering, Namdo Provincial College,
[1]Team of Compound Development, Kumho Tire Co.
(gjeon@damyang.ac.kr*)

INTRODUCTION

For a stable and long-service tire, unaged adhesion properties of the steel cord to the rubber compound should be excellent and adhesion degradation after aging treatments ought to be delayed as much as possible to maintain the function of reinforcement. Unfortunately, adhesion degradation is inevitable due to the additional growth of copper sulfide and the loss of metallic zinc in the adhesion interphase, caused by heat generated during tire use, or by contact with moisture in the air [1]. Lowering the amount of brass plating on the steel cord and reducing the copper content in the brass made remarkable improvement in adhesion stability. This was due to the suppression of an additional growth of copper sulfide and the dezincification of the adhesion layer.

Benko [2] deposited the various metals such as copper, zinc and nickel with very thin film by ion beam deposition or etching technique. Seo *et al.* [3] manufactured thin Cu/Zn film-coated steel cords (not brass-coated steel cords) as new material and plates with 30-90 nm of copper thickness. Copper was deposited on the uniform surface of a zinc-plated steel filament or plate by the substitution plating method. The adhesion properties of the Cu/Zn film-coated steel cords and its plates were depended considerably on the amount of both copper and zinc plating. The Cu/Zn film-coated steel cord, with a thin copper film of 30 nm on average, exhibited similar adhesion strength to the rubber compound compared to brass-plated steel cords, which are currently used in tires [4]. Furthermore, the Cu/Zn film-coated steel cords showed excellent adhesion stability against aging treatments. The suppression of the excessive growth of copper sulfide on the Cu/Zn film-coated steel cords, due to the limitation of the amount of copper plating, resulted in a good stability against aging treatment.

The plate is more appropriate than the cord, concerning the analysis of surface and adhesion interphase. Therefore, our group has developed nano-copper-coated iron plate prior to application of nano-copper-plated steel cord. In this study, we manufactured three kind of nano-copper-coated iron plates with copper thickness from 29 nm to 56 nm by sputtering technique. Also, brass plate was used to compare the adhesion property to rubber compound with that of nano-copper-coated iron plates. The structure of the adhesion interphases remaining on the nano-copper-coated iron plates were studied to illustrate the potential for the application of nano-copper-film as a coating material of the iron plate determined by depth profiles in AES and tapping mode in AFM.

EXPERIMENTAL

The surface of an iron plate (purity : 99.9%) with 100 mm long, 70 mm wide and 0.4 mm thick (Jungdo Testing Co., Korea) was smoothed with 4000 mesh sandpaper and cleaned by dipping it into acetone to remove grease and other contaminants. The oxide layer of the iron plate was removed by treating it with 5% sulfuric acid for 60 s. The nano-copper-film was sputtered onto iron plate treated above mentioned using CVD reactor in the sputter system (PECVD & Sputter Sys., Sam-Han Vacuum Development Co., Korea) for constant time at 10^{-4} - 10^{-5} Torr under argon plasma. The thickness of the nano-copper-film on iron plate was controlled by changing the sputter time for 5, 8 and 10 min

respectively. The average thickness of the nano-copper-film on iron plate was determined by Ar^+ sputtering of Auger electron spectroscopy. The thicknesses of the nano-copper-film were 29, 41 and 56 nm respectively. The nano-copper-coated plate was named Cu( ) plate, with the thickness in nm being the number in parentheses. Brass plate (Ohio Gasket & Shim Co., U.S.A.) with a composition of 70 wt% of Cu was used for comparison with nano-copper-coated iron plates.

A rubber compound was prepared. The formulation of the rubber compound is tabulated in Table 1. Adhesion properties were evaluated through a peel-out test. The nano-copper-coated iron plates or brass plate was sandwiched with 2 mm thick rubber pads, and they were cured at 160 ^oC and 13 MPa on a cure press. Curing was maintained for 3 min longer than t_{90} time to compensate for heat transfer. For optimum cure, adhesion samples were cured for 15 min, which is 3 min longer than t_{90} time to compensate for heat transfer. For over cure, adhesion specimens were also prepared by curing for 51 min, which is 3 min longer than four times of t_{90} time to compensate for heat transfer.

Filter paper with a pore of 5.0 ㎛ (Millipore Co., U.S.A.) was placed at the interface between a rubber pad of 2 mm and the nano-copper-coated iron plates or brass plate. Adhesion specimens were cured at 160 ^oC for 51 min. Sulfur from the rubber compound migrated through the pores of the filter paper and reacted with the copper of the nano-copper-coated iron plates or the brass plate, forming an adhesion interphase. After removing the rubber and filter paper from the metal plate, the adhesion interphase, mainly copper sulfide, remained on the metal plate. The depth profiles from the outer surface to the bulk plate were recorded on a Perkin-Elmer Auger spectrometer (model Phi 670, Perkin-Elmer Co., U.S.A.). A surface of 10 ×10 ㎛^{2} was examined using an ion beam with a potential of 5.0 ㎸, a current of 0.03 ㎂, and an incident angle of 60 ^{o} to the specimen, the same conditions described in a previously published paper. A sputter gun with an argon ion beam rastered on a 2 ×2 mm^2 area for depth profiling. The sputtering rate was determined to be 4.5 nm·min^{-1} using tantalum pentoxide plate as reference material.

Tapping mode investigations were carried out with the atomic force microscope (SPM-9500 J3, Shimaduzu Co.). The cantilever made of silicon nitride has a length of 200 μm and resonant frequency of 40 kHz. The spring constant used was 0.15 N/m. The used integrated tip has a base area of 10 x 10 μm^2 and a height between 300 and 500 nm. The software (SPM offline version 2.30, Shimadzu Co) is used to control the microscope and to evaluate the recorded data. The software allows to generate two- and three-dimensional image and distance measurements and the calculation of the RMS-roughness which is used to compare the different surface of nano-copper-coated iron plates and brass plate before and after adhesion to rubber compound.

RESULTS AND DISCUSSION

The adhesion interphases determined by AES depth profiles are shown in Figure 1. A sufficient copper sulfide in the adhesion interphase appeared in the Cu(29) plate. With increasing thickness of the Cu film in nano-copper-coated iron plates, an excess copper sulfide formed. This led to poor adhesion property. This phenomenon is explained that copper sulfide formation in the adhesion interphase formation is dominant with increasing Cu thickness.

It is well known that the reactivity of copper to sulfur is faster than that of brass to sulfur. Also, the formation of adhesion interphase during curing is much faster than that of vulcanization reaction of the rubber compound. Therefore, most of the adhesion interphase between nano-copper-coated iron plates and rubber compound may form before scorch time of the rubber compound. Therefore, the cure rate of rubber compound in the case of nano-copper-coated iron plates is more important than in the case of a brass plate.

The large difference in rates of adhesion interphase formation and vulcanization is responsible for the formation of a weak boundary layer in the thin rubber layer adjacent to the interphase. During the cure of adhesion samples, the lack of sulfur in the thin rubber layer adjacent to the interphase occurs due to large consumption of sulfur in the formation of the interphase instead of in vulcanization. Unfortunately, the diffusion of sulfur from the bulk rubber to the thin rubber layer adjacent to the interphase is effectively hindered by sulfur cross-linking network formed in the rubber during initial

vulcanization. As cure of adhesion samples proceeds, the bulk rubber is completely cured whereas the thin rubber layer adjacent to adhesion interphase does not cure sufficiently. Thus the thin rubber layer adjacent to the interphase of nano-copper-coated iron plates will have a low sulfur crosslink density compared to the bulk rubber. In principle, a thin copper coating is recommended to prevent an excessive growth of copper sulfide, but too thin Cu coating induces interfacial failure in the adhesion interphase and results in low adhesion.

The surface roughness of adhesion interphase increased with increasing copper thickness (Table 2). Compared to adhesion interphase of brass plate, the surface roughness in adhesion interphases of nano-copper-coated iron plates is significantly small indicating the formation of controlled adhesion interphase.

The two and three-dimensional image of adhesion interphases using AFM are shown for Cu(29) in Figure 2.

One of the several advantages of the copper-coated iron plate is the extremely high resistance to moisture. Since the nano-copper-coated iron plates do not contain zinc, degradation due to dezincification can be avoided.

CONCLUSIONS

The nano-copper-coated iron plates were prepared by sputtering technique and the adhesion interphases to rubber compound after cure were characterized by TM-AFM and AES depth profiles. From the analyses of AES depth profiles, the thickness of adhesion interphases to rubber compound increased with increase of copper plating to iron plate. From the surface roughness of adhesion interphases calculated from root mean square determined by TM-AFM, adhesion interphase of nano-copper-coated iron plates is significantly small compared to that of brass plate. The controlled formation of adhesion interphase in nano-copper-coated iron plate to rubber compound indicated the excellent adhesion retention and possibility of a new material to reinforce rubber compound.

ACKNOWLEDGEMENT

This work was supported by Korea Research Foundation Grant (KRF-2003-002-D00117).

REFERENCES

1. Jeon, G. S., *J. Adhesion Sci. Technol.*, **17**, 797(2003).
2. D. A. Benko, *US Patent , US 4,517,066* (1985).
3. Cho, P. L., Jeon, G. S., Ryu, S. K., Seo, G., *J. Adhesion*, **70**, 241(1999).
4. Seo, G., Cho, P. L., Jeon, G. S., Ryu, S. K., *US Patent , US 6,410,098 B1*(2002).

Table 1. Recipe of rubber compounds used

Material	Trade name	Manufacturer	Content (phr)
natural rubber	SMR-20	Lee Rubber Co., Malaysia	100
carbon black	N330	Lucky Co., Korea	60
processing oil	A#2	Michang Co., Korea	3.5
activator	ZnO	Hanil Co., Korea	8
antioxidant	Kumanox-13	Monsanto Co., U.S.A.	1
adhesion promoter	B-18S	Indspec Co., U.S.A.	2
adhesion promoter	Manobond-680C	Rhone Poulenc Co., France	0.5
activator	Stearic acid	Pyungwha Co., Korea	1.5
accelerator	DCBS	Monsanto Co., U.S.A.	0.7
sulfur	Crystex HS 20	Akzo Co., The Netherlands	5
adhesion promoter	Cyrez-964	Cytec Co., U.S.A.	3

Table 2. The changes of the rms-roughness of the scanned areas on the raw plates and adhesion interphases determined by tapping mode in AFM.

Plate	RMS (nm) of plate surface	
	Raw plate	Adhesion interphase
Cu(29) plate	14	24
Cu(41) plate	14	26
Cu(56) plate	18	42
brass plate	29	74

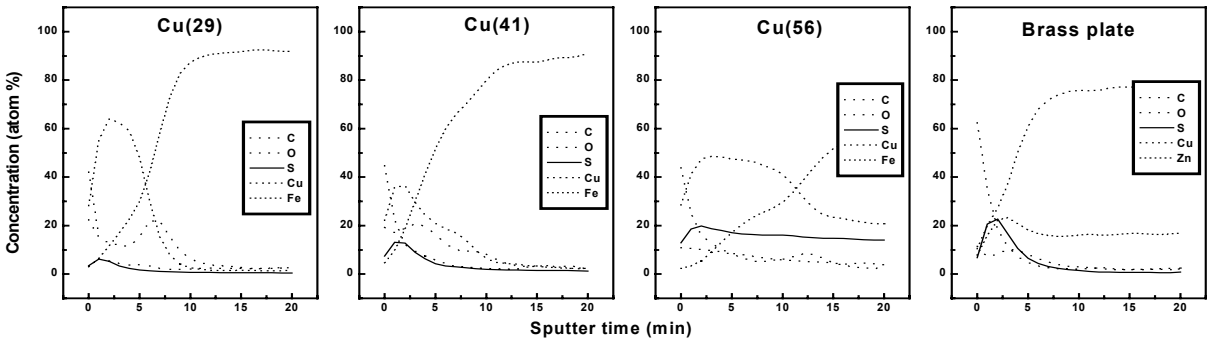

Figure 1. AES depth profiles of adhesion interphases between the nano-copper-coated iron plates and rubber compound.

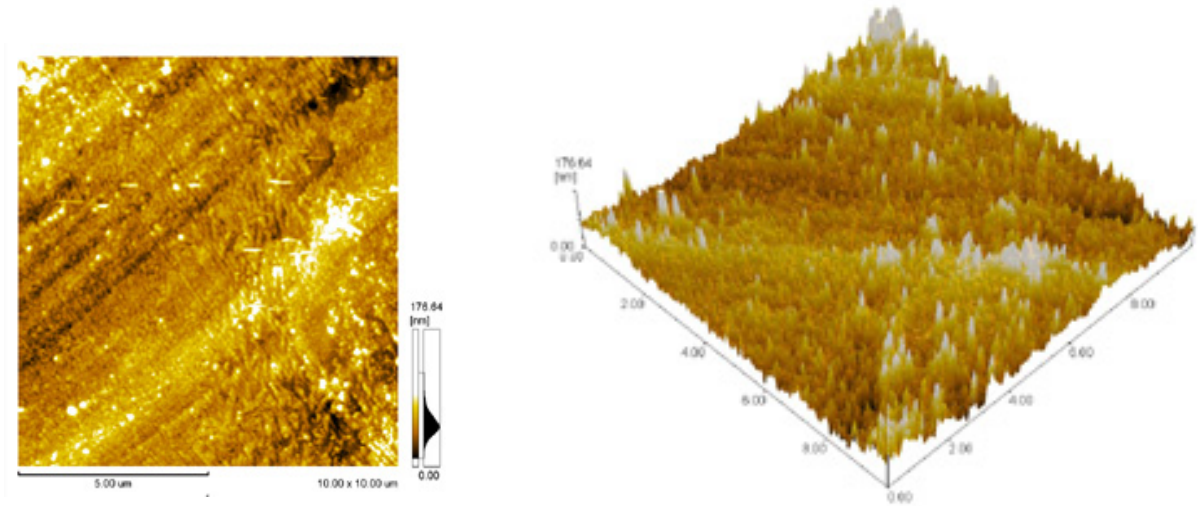

Figure 2. TM-AFM images of adhesion interphases between the nano-copper-coated iron plates and rubber compound.